AST-120 Ameliorates Lowered Exercise Capacity and Mitochondrial Biogenesis in the Skeletal Muscle from Mice with Chronic Kidney Disease via Reducing Oxidative Stress

Mikito Nishikawa, Naoki Ishimori, Shingo Takada, Akimichi Saito, Tomoyasu Kadoguchi, Takaaki Furihata, Arata Fukushima, Shouji Matsushima, Takashi Yokota, Shintaro Kinugawa, Hiroyuki Tsutsui

Department of Cardiovascular Medicine, Hokkaido University Graduate School of Medicine, Sapporo, Japan

Running title: Exercise Capacity and AST-120

Address for correspondence: Naoki Ishimori, MD, PhD.
Department of Cardiovascular Medicine
Hokkaido University Graduate School of Medicine
Kita-15, Nishi-7, Kita-ku, Sapporo 060-8638, Japan
Phone: +81-11-706-6973
Fax: +81-11-706-7874
E-mail: ishimori@med.hokudai.ac.jp

Key words: AST-120, chronic kidney disease, exercise capacity, indoxyl sulfate, mitochondria, skeletal muscle

Short summary

The administration of an oral adsorbent, AST-120, into subtotal-nephrectomized mice improved their exercise capacity and mitochondrial biogenesis of the skeletal muscle by reducing the oxidative stress induced by indoxyl sulfate.

Abstract

Background. Exercise capacity and quality of life are markedly impaired in chronic kidney disease (CKD). Increased plasma uremic toxins such as indoxyl sulfate (IS), which induce oxidative stress, may be involved in this process. An oral adsorbent, AST-120, can reduce circulating IS, however, its effects on skeletal muscle and exercise capacity have not been investigated in CKD.

Methods. Subtotal-nephrectomy or sham operation was performed in 8-week-old C57BL/6J mice. They were divided into 2 groups with or without 8% (w/w) of AST-120 in standard diet for 20 weeks. Sham, Sham+AST-120, CKD, and CKD+AST-120 (n=12, each group) were studied. We also conducted a C2C12 cell culture study to determine the direct effects of IS on oxidative stress.

Results. Plasma IS levels were significantly increased in CKD compared to Sham (1.05±0.11 vs. 0.21±0.03 mg/dL, $P<0.05$), which was significantly ameliorated in CKD+AST-120 (0.41±0.06 mg/dL). The running distance to exhaustion determined by treadmill tests was significantly reduced in CKD compared to Sham (267±17 vs. 427±36 m, $P<0.05$), and this reduction was also significantly ameliorated in CKD+AST-120 (407±38 m) without altering skeletal muscle weight. Citrate synthase activity and mitochondrial biogenesis gene were down regulated and superoxide production was significantly increased in the skeletal muscle from CKD, and these changes were normalized in CKD+AST-120. Incubation of C2C12 cells with IS significantly increased NAD(P)H oxidase activity.

Conclusions. The administration of AST-120 improved exercise capacity and mitochondrial biogenesis of skeletal muscle via reducing oxidative stress. AST-120 may be a novel therapeutic agent against exercise intolerance in CKD.

(248 words/ 250 words limit)

Introduction

Chronic kidney disease (CKD) is a common disorder; its prevalence exceeds 10% of the population in many countries [1]. Skeletal muscle function is impaired in CKD patients and leads to lowered exercise capacity [2, 3]. Lowered exercise capacity is an independent predictor of mortality in patients with CKD, because it promotes a sedentary lifestyle leading to adverse complications such as cardiovascular disease [4, 5]. Favorable effects of aerobic exercise training on exercise intolerance in CKD patients were reported, however it is difficult for bedridden and wheelchair-bound patients to engage in such exercise [6, 7]. Therefore a development of pharmacological intervention which specifically improves the exercise capacity of CKD patients is required.

Exercise capacity depends on various factors including cardiac function, hemoglobin concentration, skeletal muscle capillary, and skeletal muscle function [8]. The mechanisms of exercise intolerance in CKD are multifactorial, including impaired perfusion due to chronic heart failure, decreased oxygen supply to skeletal muscle due to renal anemia and decreased skeletal muscle capillaries, skeletal muscle atrophy due to insulin resistance, inactivity, and activation of the renin-angiotensin system (RAS) [9-13]. In addition, recent reports showed that the mitochondrial function of skeletal muscle is impaired in both patients and an animal model of CKD [14-16]. Elevated uremic toxins inducing oxidative stress may impair the mitochondria function of skeletal muscle and lead to exercise intolerance in CKD, however the effects of uremic toxins on skeletal muscle function have not been elucidated [17].

Indoxyl sulfate (IS) is one of major uremic toxins which accumulate in CKD patients and impairs organ function by inducing oxidative stress [18-20]. *In vitro* analysis showed that IS induces oxidative stress via the activation of NAD(P)H oxidase in various types of cells [21-23]. An oral adsorbent, AST-120, reduces circulating IS by adsorbing indole, a precursor

of IS in the intestines [18]. It exerts organ protective effects via reduction of oxidative stress [20, 24, 25], however the effects of AST-120 on skeletal muscle have not been reported. We have demonstrated that enhanced oxidative stress in the skeletal muscle is involved in the impaired mitochondrial function and lowered exercise capacity in type 2 diabetic mice [26]. We thus hypothesized that AST-120 could improve the impaired mitochondrial function of skeletal muscle and the lowered exercise capacity in CKD by suppressing increased oxidative stress. Here, we determined whether AST-120 could improve the exercise capacity, mitochondrial function, and oxidative stress of skeletal muscle in subtotal-nephrectomized CKD mice. Furthermore, to verify whether IS activates NAD(P)H oxidase in skeletal muscle, we conducted a C2C12 cell culture study.

Materials and methods

All procedures and animal care were approved by our institutional animal research committee and conformed to the guidelines for the Care and Use of Laboratory Animals at the Hokkaido University Graduate School of Medicine kept in accordance with relevant national and international guidelines.

Experimental animals

Male 6- to 7-week-old C57BL/6J mice (Charles River Japan, Yokohama, Japan) were weaned onto a pulverized standard diet (SD). At 8 weeks of age, the mice were randomized to either develop CKD by a two-step surgical subtotal-nephrectomy or serve as sham-operated controls (Sham) as described previously [27]. In brief, the upper and lower poles of the right kidney were resected leaving an intact kidney segment. Two weeks later, the left kidney was removed after ligation of the renal blood vessels and the ureter under anesthesia. At 11 weeks of age, each group of mice was further divided into 2 groups with or without 8% (w/w) of AST-120 (Kremezin®; Kureha Pharmaceuticals, Tokyo, Japan) in SD. The concentration of AST-120 was chosen on the basis of previous studies [24, 28].

The present study was performed in the following 4 groups of mice; 1) Sham (n=12), 2) Sham+AST-120 (n=12), 3) CKD (n=12), and 4) CKD+AST-120 (n=12). These procedures were performed using numeric codes to identify the animals. At 28-30 weeks of age, exercise test, intraperitoneal glucose tolerance test and echocardiographic measurements were performed. After that, all mice were euthanized, blood samples were collected, and organ weights were measured.

Anesthesia

Mice were anaesthetized with intraperitoneal injection of mixture of medetomidine hydrochloride (0.15 mg/kg; Kyoritsu Seiyaku, Tokyo, Japan), midazolam (2 mg/kg; Astellas Pharma Inc., Tokyo, Japan), and butorphanol (2.5 mg/kg; Meiji Seika Pharma Co., Ltd., Tokyo, Japan), and its adequacy was monitored from the disappearance of the pedal withdrawal reflex [29].

Blood biochemical measurements

Blood samples were collected from the inferior vena cava at the time of euthanasia and stored at −80°C. Plasma levels of blood urea nitrogen (BUN) were measured using the QuantiChrom Urea Assay Kit (Bioassay Systems, Hayward, CA, USA). Plasma levels of angiotensin II (Ang II) were measured using the EIA kit (Peninsula Laboratories, Inc., San Carlos, CA, USA). Plasma levels of IS were measured by high performance liquid chromatography as previously described [30]. Total cholesterol, non-esterified fatty acid (NEFA), triglyceride, and hemoglobin were measured by the Cholesterol E-test, NEFA C-test, Triglyceride E-test and Hemoglobin B-test, respectively (Wako Pure Chemical Industries, Osaka, Japan).

For the glucose or insulin tolerance test, mice were fasted for 6 h and given an intraperitoneal injection of glucose (1 mg/g body weight) or human regular insulin (0.5 mU/g body weight) in purified water. Blood samples were repeatedly drawn from the tail vein of the same mice before and 15, 30, 60, 90, and 120 min after the injection. Blood glucose levels were determined using a glucometer (Glutest Ace R; Sanwa Kagaku Kenkyusho, Nagoya, Japan).

Blood lactate levels were determined using one drop of blood obtained from the mouse's tail at the end of treadmill test [31]. The lactate concentration was assayed using a portable

lactate blood analyzer (Lactate Pro LT; Arkray, Kyoto, Japan) according to the manufacturer's instructions.

Echocardiographic and blood pressure measurements

Echocardiographic measurements were obtained under light anesthesia with using previously described method [32, 33]. Systemic blood pressure was measured using the tail-cuff method (BP-98A; Softron, Tokyo, Japan) without anesthesia.

Exercise capacity and spontaneous physical activity

Mice were treadmill-tested to measure indexes defining whole body exercise capacity as previously described [26]. At the time of the treadmill testing, each mouse was forced to run on a motor-driven treadmill (Oxymax 2; Columbus Instruments, Columbus, OH, USA). Basal measurements were obtained over a period of 10 min. The mouse was then provided with a 10 min warm-up period at 6 m/min at 0° inclination. After the mouse warmed up, the angle was fixed at 10° and the speed was incrementally increased by 2 m/min every 2 min until the mouse reached exhaustion. Exhaustion was defined as spending time (10 sec) on the shocker plate without attempting to reengage the treadmill. The work was defined as the product of the vertical running distance to exhaustion and body weight.

Spontaneous physical activity was measured using an animal movement analysis system (Actimo System; Shintechno, Fukuoka, Japan) as previously described [34].

Histology and biochemical analyses of the skeletal muscle

Hindlimb skeletal muscle was excised, fixed in 4% paraformaldehyde, embedded in paraffin, and stained with hematoxylin-eosin (HE) for histological analysis. A morphological analysis of the cell cross-sectional area was performed in at least 50 cells from each mouse

[31]. To evaluate angiogenesis, we performed immunohistochemistry for CD31 (Dako, Glostrup, Denmark) and counted the number of CD31-positive cells.

For immunoblotting, hindlimb skeletal muscle tissue samples were lysed and cell lysates (50 μg) were then electrophoretically separated as previously described [31]. After transferred onto polyvinylidene difluoride membranes, the membranes were incubated overnight at 4°C with primary antibodies (dilution 1:1,000) against Gαq protein (Cell Signaling, Danvers, MA, USA) and angiotensin II type 1 receptor (AT1R; Santa Cruz Biotechnology, Santa Cruz, CA, USA). Horseradish peroxidase-conjugated secondary antibodies were used for the secondary detection (dilution 1:5,000; Santa Cruz). After incubation with secondary antibodies, reactive bands were detected using the chemiluminescence detection reagent ECL™ Western Blotting Analysis System (GE Healthcare, Amersham, UK). Equal loading of protein was verified by immunoblotting with GAPDH (Cell Signaling). Quantification of protein levels was performed with Image J (National Institutes of Health, Bethesda, MD, USA).

For quantitative reverse transcription-polymerase chain reaction (qRT-PCR), total RNA was extracted from the hindlimb skeletal muscle tissues with QuickGene-810 (FujiFilm, Tokyo, Japan) according to the manufacturer's instructions. cDNA was synthesized with a high-capacity cDNA reverse transcription kit (Applied Biosystems, Foster City, CA, USA). TaqMan quantitative PCR was performed with the 7300 real-time PCR system (Applied Biosystems) to amplify samples for peroxisome proliferator-activated receptor gamma coactivator-1alpha (PGC-1α, Mm01208835_m1), ATP synthase (Mm00443967_gl), cytochrome c oxidase subunit IV (COX IV, Mm01250094_ml), ATP synthase (Mm00443967_gl), cytochrome c oxidase subunit IV (COX IV, Mm01250094_ml), BCL2/adenovirus E1B 19 kDa protein-interacting protein 3-like (BNIP3L, Mm00786306_s1), PTEN-induced putative kinase (PINK1, Mm00550827_m1), $p22^{phox}$ (Mm00514478_m1), Nox2 (Mm01287743_ml), $p47^{phox}$ (Mm00447921_ml), $p67^{phox}$ (Mm00726636_ml), $p40^{phox}$

(Mm00476300_ml), and Rac-1 (Mm01201653_mH). These transcripts were normalized to GAPDH. All primers were purchased from Applied Biosystems. Data were analyzed using a comparative $2^{-\Delta\Delta CT}$ method.

Measurement of mitochondrial function and oxidative stress

The enzymatic activity of citrate synthase (CS, a key enzyme of tricarboxylic acid cycle) was spectrophotometrically determined in the tissue homogenate from a skeletal muscle sample and in the mitochondria isolated from skeletal muscle, as previously described [35]. The specific enzymatic activities of mitochondrial electron transport chain (ETC) complex I (rotenone-sensitive NADH-ubiquinone oxidoreductase), complex II (succinate-ubiquinone oxidoreductase), complex III (ubiquinol-cytochrome c oxidoreductase), and complex IV (cytochrome c oxidase) were measured in the mitochondria isolated from skeletal muscle as previously described [36].

To evaluate superoxide production in the skeletal muscle, the chemiluminescence elicited by superoxide in the presence of lucigenin (5 μmol/L) was measured using a luminometer (AccuFLEX Lumi 400; Aloka, Tokyo, Japan) as previously described [26].

Transmission electron microscopy

The skeletal muscle samples were fixed in 2% glutaraldehyde with phosphate buffer and post-fixed in 2% osmium tetra-oxide for 3 hours in the ice bath. The samples were then serially dehydrated in a graded ethanol and embedded in epoxy resin. Ultrathin sections were obtained by ultramicrotome technique. The ultrathin sections stained with 2% uranyl acetate and lead citrate were then submitted to electron microscopic observation (JEM-1200EX; JEOL, Tokyo, Japan).

Cell culture studies

Mouse C2C12 myoblast cell line was obtained from the American Type Culture Collection (Manassas, VA, USA) and grown in Dulbecco's Modified Eagle's Medium (DMEM, 4.5 g glucose/L; Sigma, St. Louis, MO, USA), containing 10% fetal bovine serum, 100 IU/mL penicillin, and 100 IU/mL streptomycin in a humidified incubator at 37°C with 5% CO_2 in air. Confluent C2C12 myoblasts were differentiated into myotubes by incubation with DMEM containing 2% horse serum for 4-5 days. After differentiation, C2C12 myotubes were incubated with media containing 4% bovine serum albumin (BSA) and different concentrations of IS (Sigma) for 24 h. The doses of IS were determined in accordance with previous studies using cultured cells [37]. After 24 h incubation, the C2C12 myotubes were harvested and stored at −80°C for the measurement of NAD(P)H oxidase activity and the PCR analysis. NAD(P)H oxidase activity in C2C12 myotubes was measured by a lucigenin assay after the addition of NAD(P)H (300 μmol/L), as previously described [26].

Statistical analysis

Data are expressed as means ± SE. The statistical analyses were performed using the Student *t*-tests or an analysis of variance (ANOVA) with Tukey's post-hoc test (GraphPad Prism 5; GraphPad Software, San Diego, CA, USA). A value of $P<0.05$ was considered statistically significant.

Results

Animal characteristics

Table 1 shows the animal characteristics in 4 groups of mice at 28-30 weeks of age at sacrifice. There were no differences in the body weight, heart weight, skeletal muscle weights (including quadriceps, gastrocnemius, and soleus), systolic blood pressure, and heart rate among 4 groups. Plasma BUN levels were increased by 2.0-folds in CKD compared to Sham, but were not affected by AST-120. In contrast, plasma IS levels were significantly increased in CKD compared to Sham, and this increase was significantly ameliorated by AST-120 (**Figure 1**). Plasma total cholesterol was also increased in CKD, but was not affected by AST-120. Plasma NEFA, triglyceride, fasting glucose, and hemoglobin were comparable among 4 groups. Echocardiographic data were also comparable among 4 groups (**Supplemental Table 1**). Additionally, there was no significant difference in the area under the curve (AUC) of glucose responses after glucose load or insulin load among 4 groups (**Supplemental Figure 1A and B**).

Exercise capacity

The work, the running distance, and the run time to exhaustion determined by the treadmill tests were significantly reduced in CKD compared to Sham, and these reductions were significantly ameliorated in CKD+AST-120 (**Figure 2A-C**). Spontaneous physical activity was comparable among 4 groups of mice (**Figure 2D**).

Blood and skeletal muscle RAS

Plasma Ang II levels were higher in CKD than in Sham, and were not affected by AST-120 (**Supplemental Figure 2A**). Protein levels of AT1R and Gαq also did not differ in the skeletal muscle among 4 groups (**Supplemental Figure 2B and C**).

Histology of the skeletal muscle

Figure 3A shows representative images of skeletal muscle tissue sections stained with HE. There was no difference in the muscle cross-sectional area among 4 groups (**Figure 3B**). Immunostaining with CD31, a marker of vascular endothelial cells, for the evaluation of angiogenesis demonstrated that there was also no difference in $CD31^+$ capillary density among 4 groups (**Supplemental Figure 3A and B**).

Mitochondrial function in the skeletal muscle

The blood lactate level corrected by work, an indicator of anaerobic metabolism, was significantly increased in CKD compared to Sham, and this increase was ameliorated in CKD+AST-120 (**Figure 4A**). CS activity in the whole skeletal muscle was significantly reduced in CKD and this decrease was significantly ameliorated in CKD+AST-120 (**Figure 4B**). In contrast, CS activity in the isolated mitochondria from skeletal muscle did not differ among 4 groups of mice (**Figure 4C**). There were also no significant differences in mitochondrial ETC complex I, II, III and IV activities from the isolated skeletal mitochondria among 4 groups (**Figure 4D**).

Mitochondrial biogenesis and oxidative stress in the skeletal muscle

Gene expression of PGC-1α, which controls mitochondrial biogenesis, and ATP synthase, which is a component of mitochondrial ETC, were significantly decreased in the skeletal muscle from CKD, and these decreases were ameliorated in CKD+AST-120 (**Figure**

5A and B). Gene expression of COX IV, a component of mitochondrial ETC, was significantly decreased in the skeletal muscle in CKD, and the decrease tended to be ameliorated in CKD-AST-120, which, however, did not reach statistical significance (**Figure 5C**). There were no significant differences in gene expression of BNIP3L and PINK1, which control mitochondrial degradation, among 4 groups (data not shown).Transmission electron microscopy showed that the mitochondrial density in the skeletal muscle was decreased in CKD and this decrease was ameliorated in CKD+AST-120 (**Figure 5D**). Superoxide production determined by lucigenin chemiluminescence was significantly increased in isolated skeletal muscle from CKD and this increase was significantly reduced in CKD+AST-120 (**Figure 6**).

Effects of indoxyl sulfate on oxidative stress and mitochondria in the C2C12 cells

The exposure of IS to C2C12 cells with media containing 4% BSA significantly increased gene expression of NAD(P)H oxidase subunits, including $p22^{phox}$, Nox2, $p47^{phox}$, and $p40^{phox}$ in a dose-dependent manner (**Figure 7A-D**). Gene expression of $p67^{phox}$ and Rac1 were increased by the incubation with IS, which, however, did not reach statistical significance (**Figure 7E-F**). Similarly, the exposure of IS to C2C12 cells significantly increased NAD(P)H oxidase activity and decreased gene expression of PGC-1α at the concentration of 10 mg/dL, which is comparable to the serum levels in hemodialysis patients (**Figure 7G and H**) [23, 38, 39].

Discussion

The present study demonstrated that CKD mice showed lowered exercise capacity and increased plasma IS levels. They had impaired mitochondrial biogenesis and enhanced oxidative stress in the skeletal muscle. Importantly, the administration of AST-120 to CKD mice improved exercise capacity and mitochondrial biogenesis of the skeletal muscle in association with reducing oxidative stress. Furthermore, the exposure of IS to C2C12 cells increased NAD(P)H oxidase activity. Therefore, IS might be involved in the development of lowered exercise capacity and decreased mitochondrial biogenesis in CKD.

Major finding of the present study was that the administration of AST-120 into CKD mice improved their exercise intolerance. Furthermore, AST-120 ameliorated decreased mitochondrial biogenesis in skeletal muscle from CKD mice without affecting skeletal muscle mass and angiogenesis, which regulate exercise tolerance. CS activity, an indicator of mitochondrial quantity and function, was significantly reduced and this reduction was ameliorated by the administration of AST-120 in the whole skeletal muscle (**Figure 4B**). Additionally, mitochondrial density evaluated by electron microscopy, in addition to the gene expression of COX IV and ATP synthase, were significantly decreased in skeletal muscle from CKD mice and these decreases were ameliorated by the administration of AST-120 (**Figure 5B-D**). In parallel, gene expression of PGC-1α, vital inducer of mitochondria, was decreased in the skeletal muscle from CKD mice and this decrease was significantly ameliorated by AST-120, while mitochondrial complex I-IV activities did not differ among the groups (**Figure 4D and 5A**). These data suggested that administration of AST-120 ameliorated the decreased mitochondrial quantity through the improvement of mitochondrial biogenesis. These results are consistent with previous studies, in which the mitochondrial

quantity of skeletal muscle was decreased in patients and an animal model of CKD, leading to exercise intolerance [14-16].

Our previous study demonstrated that oxidative stress in skeletal muscle substantially impaired mitochondrial function and limited exercise capacity in type 2 diabetic mice [26]. In the present study, superoxide production was increased also in skeletal muscle from CKD mice and this elevation was ameliorated by the administration of AST-120 (**Figure 6**). These results suggest that an elevation of IS in CKD mice induces superoxide production and may impair mitochondrial biogenesis in the skeletal muscle. Our cell culture study further confirmed that IS increased NAD(P)H oxidase activity and reduced the gene expression of PGC-1α in C2C12 cells at the same concentrations as observed in hemodialysis patients (**Figure 7**) [23, 38, 39].

In the present study, mice were subtotally nephrectomized to induce renal failure and their plasma levels of BUN increased at the levels as previously reported [40]. However, skeletal muscle weight and cross-sectional area of muscle cells did not differ between CKD and Sham mice, indicating that skeletal muscle atrophy was not observed in our CKD mice (**Figure 3, Table 1**). These results are consistent with the previous study by Tamaki *et al.* reported in which skeletal muscle atrophy was not observed at an early phase after subtotal-nephrectomy, despite lowered exercise capacity and impaired mitochondrial function [16]. However, they found skeletal muscle atrophy in CKD mice 1 year after subtotal-nephrectomy, indicating that functional muscle dysfunction such as exercise intolerance preceded histological muscle degeneration in CKD.

There are several limitations of which should be acknowledged in this study. First, IS is recognized as one of the most potent uremic toxin, and AST-120 is an oral adsorbent. Therefore, we could not exclude the possibility that the beneficial effects of AST-120 on exercise capacity may depend on the reduction of other uremic toxins which can be reduced

by AST-120. Second, the cause-and-effect relationship between IS and oxidative stress as well as mitochondrial dysfunction has not been directly proved in our animal model of CKD. However, the cell culture study of C2C12 cells suggested that IS could directly induce oxidative stress via NAD(P)H oxidase and impair mitochondrial function. Third, recently, Vaziri *et al.* reported that urea and urea-derived ammonia altered the colonic bacterial flora and impaired the colonic epithelial barrier structure, resulting in formation and influx of uremic toxins in CKD animals and patients [41, 42]. They also reported that the administration of AST-120 ameliorated oxidative stress by adsorbing urea and ammonia and protecting the epithelial barrier structure [43]. Therefore, the beneficial effects of AST-120 on the reduction of oxidative stress may depend on the protection of the colonic epithelial barrier structure. Fourth, our administration of AST-120 to CKD mice significantly improved exercise capacity at an early phase after subtotal-nephrectomy, however, the effects of AST-120 on skeletal muscle atrophy remain further to be elucidated.

In conclusion, the administration of AST-120 to CKD mice improved their exercise capacity and mitochondrial biogenesis of their skeletal muscle by reducing the oxidative stress induced by IS. AST-120 may be an effective novel therapeutic agent against exercise intolerance in CKD patients.

Acknowledgements

We thank Akiko Aita, Miwako Fujii, Noriko Ikeda, and Yuki Kimura for excellent technical assistance.

Sources of Funding

This work was supported in part by grants from the Ministry of Education, Science, and Culture (23591056), Mitsubishi Pharma Research Foundation, and Research Foundation for Community Medicine.

Conflict of interest statement

The authors have no financial conflict of interest regarding this manuscript.

References

1. James MT, Hemmelgarn BR, Tonelli M. Early recognition and prevention of chronic kidney disease. Lancet 2010; 375: 1296-1309
2. Fried LF, Lee JS, Shlipak M, *et al.* Chronic kidney disease and functional limitation in older people: health, aging and body composition study. J Am Geriatr Soc 2006; 54: 750-756
3. Reese PP, Cappola AR, Shults J, *et al.* Physical performance and frailty in chronic kidney disease. Am J Nephrol 2013; 38: 307-315
4. Sietsema KE, Amato A, Adler SG, *et al.* Exercise capacity as a predictor of survival among ambulatory patients with end-stage renal disease. Kidney Int 2004; 65: 719-724
5. Roshanravan B, Khatri M, Robinson-Cohen C, *et al.* A prospective study of frailty in nephrology-referred patients with CKD. Am J Kidney Dis 2012; 60: 912-921
6. Storer TW, Casaburi R, Sawelson S, *et al.* Endurance exercise training during haemodialysis improves strength, power, fatigability and physical performance in maintenance haemodialysis patients. Nephrol Dial Transplant 2005; 20: 1429-1437
7. Wang XH, Mitch WE. Mechanisms of muscle wasting in chronic kidney disease. Nat Rev Nephrol 2014; 10: 504-516
8. Joyner MJ, Coyle EF. Endurance exercise performance: the physiology of champions. J Physiol 2008; 586: 35-44
9. Fahal IH. Uraemic sarcopenia: aetiology and implications. Nephrol Dial Transplant 2014; 29: 1655-1665
10. Baraldi E, Montini G, Zanconato S, *et al.* Exercise tolerance after anaemia correction with recombinant human erythropoietin in end-stage renal disease. Pediatr Nephrol 1990; 4: 623-626

11. Flisinski M, Brymora A, Elminowska-Wenda G, *et al.* Influence of different stages of experimental chronic kidney disease on rats locomotor and postural skeletal muscles microcirculation. Ren Fail 2008; 30: 443-451
12. Bailey JL, Zheng B, Hu Z, *et al.* Chronic kidney disease causes defects in signaling through the insulin receptor substrate/phosphatidylinositol 3-kinase/Akt pathway: implications for muscle atrophy. J Am Soc Nephrol 2006; 17: 1388-1394
13. Sakkas GK, Sargeant AJ, Mercer TH, *et al.* Changes in muscle morphology in dialysis patients after 6 months of aerobic exercise training. Nephrol Dial Transplant 2003; 18: 1854-1861
14. Adey D, Kumar R, McCarthy JT, *et al.* Reduced synthesis of muscle proteins in chronic renal failure. Am J Physiol Endocrinol Metab 2000; 278: E219-225
15. Yazdi PG, Moradi H, Yang JY, *et al.* Skeletal muscle mitochondrial depletion and dysfunction in chronic kidney disease. Int J Clin Exp Med 2013; 6: 532-539
16. Tamaki M, Miyashita K, Wakino S, *et al.* Chronic kidney disease reduces muscle mitochondria and exercise endurance and its exacerbation by dietary protein through inactivation of pyruvate dehydrogenase. Kidney Int 2014; 85: 1330-1339
17. Yokoi H, Yanagita M. Decrease of muscle volume in chronic kidney disease: the role of mitochondria in skeletal muscle. Kidney Int 2014; 85: 1258-1260
18. Niwa T. Role of indoxyl sulfate in the progression of chronic kidney disease and cardiovascular disease: experimental and clinical effects of oral sorbent AST-120. Ther Apher Dial 2011; 15: 120-124
19. Yisireyili M, Shimizu H, Saito S, *et al.* Indoxyl sulfate promotes cardiac fibrosis with enhanced oxidative stress in hypertensive rats. Life Sci 2013; 92: 1180-1185
20. Nakagawa N, Hasebe N, Sumitomo K, *et al.* An oral adsorbent, AST-120, suppresses oxidative stress in uremic rats. Am J Nephrol 2006; 26: 455-461

21. Gelasco AK, Raymond JR. Indoxyl sulfate induces complex redox alterations in mesangial cells. Am J Physiol Renal Physiol 2006; 290: F1551-1558

22. Dou L, Jourde-Chiche N, Faure V, *et al.* The uremic solute indoxyl sulfate induces oxidative stress in endothelial cells. J Thromb Haemost 2007; 5: 1302-1308

23. Muteliefu G, Enomoto A, Jiang P, *et al.* Indoxyl sulphate induces oxidative stress and the expression of osteoblast-specific proteins in vascular smooth muscle cells. Nephrol Dial Transplant 2009; 24: 2051-2058

24. Fujii H, Nishijima F, Goto S, *et al.* Oral charcoal adsorbent (AST-120) prevents progression of cardiac damage in chronic kidney disease through suppression of oxidative stress. Nephrol Dial Transplant 2009; 24: 2089-2095

25. Yu M, Kim YJ, Kang DH. Indoxyl sulfate-induced endothelial dysfunction in patients with chronic kidney disease via an induction of oxidative stress. Clin J Am Soc Nephrol 2011; 6: 30-39

26. Yokota T, Kinugawa S, Hirabayashi K, *et al.* Oxidative stress in skeletal muscle impairs mitochondrial respiration and limits exercise capacity in type 2 diabetic mice. Am J Physiol Heart Circ Physiol 2009; 297: H1069-1077

27. Phan O, Ivanovski O, Nikolov IG, *et al.* Effect of oral calcium carbonate on aortic calcification in apolipoprotein E-deficient (apoE-/-) mice with chronic renal failure. Nephrol Dial Transplant 2008; 23: 82-90

28. Lekawanvijit S, Kompa AR, Manabe M, *et al.* Chronic kidney disease-induced cardiac fibrosis is ameliorated by reducing circulating levels of a non-dialysable uremic toxin, indoxyl sulfate. PLoS One 2012; 7: e41281

29. Kawai S, Takagi Y, Kaneko S, *et al.* Effect of three types of mixed anesthetic agents alternate to ketamine in mice. Exp Anim 2011; 60: 481-487

30. Adijiang A, Goto S, Uramoto S, *et al.* Indoxyl sulphate promotes aortic calcification with expression of osteoblast-specific proteins in hypertensive rats. Nephrol Dial Transplant 2008; 23: 1892-1901

31. Takada S, Kinugawa S, Hirabayashi K, *et al.* Angiotensin II receptor blocker improves the lowered exercise capacity and impaired mitochondrial function of the skeletal muscle in type 2 diabetic mice. J Appl Physiol 2013; 114: 844-857

32. Matsushima S, Kinugawa S, Yokota T, *et al.* Increased myocardial NAD(P)H oxidase-derived superoxide causes the exacerbation of postinfarct heart failure in type 2 diabetes. Am J Physiol Heart Circ Physiol 2009; 297: H409-416

33. Sobirin MA, Kinugawa S, Takahashi M, *et al.* Activation of natural killer T cells ameliorates postinfarct cardiac remodeling and failure in mice. Circ Res 2012; 111: 1037-1047

34. Chikahisa S, Tominaga K, Kawai T, *et al.* Bezafibrate, a peroxisome proliferator-activated receptors agonist, decreases body temperature and enhances electroencephalogram delta-oscillation during sleep in mice. Endocrinology 2008; 149: 5262-5271

35. Suga T, Kinugawa S, Takada S, *et al.* Combination of exercise training and diet restriction normalizes limited exercise capacity and impaired skeletal muscle function in diet-induced diabetic mice. Endocrinology 2014; 155: 68-80

36. Takada S, Hirabayashi K, Kinugawa S, *et al.* Pioglitazone ameliorates the lowered exercise capacity and impaired mitochondrial function of the skeletal muscle in type 2 diabetic mice. Eur J Pharmacol 2014; 740: 690-696

37. Tumur Z, Niwa T. Indoxyl sulfate inhibits nitric oxide production and cell viability by inducing oxidative stress in vascular endothelial cells. Am J Nephrol 2009; 29: 551-557

38. Niwa T, Ise M. Indoxyl sulfate, a circulating uremic toxin, stimulates the progression of glomerular sclerosis. J Lab Clin Med 1994; 124: 96-104

39. Niwa T, Miyazaki T, Tsukushi S, *et al.* Accumulation of indoxyl-beta-D-glucuronide in uremic serum: suppression of its production by oral sorbent and efficient removal by hemodialysis. Nephron 1996; 74: 72-78

40. Leelahavanichkul A, Yan Q, Hu X, *et al.* Angiotensin II overcomes strain-dependent resistance of rapid CKD progression in a new remnant kidney mouse model. Kidney Int 2010; 78: 1136-1153

41. Vaziri ND, Yuan J, Rahimi A, *et al.* Disintegration of colonic epithelial tight junction in uremia: a likely cause of CKD-associated inflammation. Nephrol Dial Transplant 2012; 27: 2686-2693

42. Wong J, Piceno YM, Desantis TZ, *et al.* Expansion of urease- and uricase-containing, indole- and p-cresol-forming and contraction of short-chain fatty acid-producing intestinal microbiota in ESRD. Am J Nephrol 2014; 39: 230-237

43. Vaziri ND, Yuan J, Khazaeli M, *et al.* Oral activated charcoal adsorbent (AST-120) ameliorates chronic kidney disease-induced intestinal epithelial barrier disruption. Am J Nephrol 2013; 37: 518-525

Figure legends

FIGURE 1: Plasma levels of indoxyl sulfate (IS) in 4 groups of Sham, Sham+AST-120, CKD, and CKD+AST-120 mice (n=12 for each group). Data are expressed as means ± SE. **P*<0.05 vs. Sham; †*P*<0.05 vs. CKD. CKD, chronic kidney disease.

FIGURE 2: Exercise capacity. (**A**) The work, (**B**) run distance, and (**C**) run time to exhaustion in 4 groups of Sham, Sham+AST-120, CKD, and CKD+AST-120 mice (n=12 for each group). (**D**) Spontaneous physical activity in the 4 groups of mice (n=8 for each group). Data are expressed as means ± SE. **P*<0.05 vs. Sham; †*P*<0.05 vs. CKD.

FIGURE 3: (**A**) Representative high-power photomicrographs of skeletal muscle tissue sections stained with hematoxylin-eosin staining and (**B**) the summarized data of muscle cross-sectional area from 4 groups of Sham, Sham+AST-120, CKD, and CKD+AST-120 mice (n=6 for each group). Scale bar=100 μm. Data are expressed as means ± SE.

FIGURE 4: Mitochondrial function. (**A**) Blood lactate level after exercise corrected by work from 4 groups of Sham, Sham+AST-120, CKD, and CKD+AST-120 mice (n=12 for each group). (**B** and **C**) Citrate synthase (CS) activity in the whole skeletal muscle and the isolated skeletal mitochondria (n=9-11 for each group) from 4 groups of mice. (**D**) Mitochondrial electron transport chain (ETC) complex I, II, III, and IV enzymatic activities in the isolated skeletal mitochondria (n=10-12 for each group) from 4 groups of mice. Data are expressed as means ± SE. **P*<0.05 vs. Sham; †*P*<0.05 vs. CKD.

FIGURE 5: Mitochondrial biogenesis. (**A-C**) Gene expression of PGC-1α, ATP synthase, and COX IV in the skeletal muscle from 4 groups of mice (n=12 for each group). (**D**) Transmission electron microscopic images of the skeletal muscle from 4 groups of mice. Arrows: mitochondria, scale bar=2 μm. Data are expressed as means ± SE. **P*<0.05 vs. Sham; †*P*<0.05 vs. CKD. PGC-1α, peroxisome proliferator-activated receptor gamma coactivator 1α. COX IV, cytochrome c oxidase subunit IV.

FIGURE 6: Superoxide production in the skeletal muscle from 4 groups of Sham, Sham+AST-120, CKD, and CKD+AST-120 mice (n=6-7 for each group). Data are expressed as means ± SE. **P*<0.05 vs. Sham; †*P*<0.05 vs. CKD.

FIGURE 7: (**A-F**) Gene expression of NAD(P)H oxidase subunits including $p22^{phox}$, Nox 2, $p47^{phox}$, $p40^{phox}$, $p67^{phox}$, Rac1 in C2C12 myotubes exposed to IS (0, 5, 10, or 20 mg/dL, for 24 h) with media containing 4% BSA. (**G**) NAD(P)H oxidase activity in C2C12 myotubes exposed to IS (0 or 10 mg/dL, for 24 h) with media containing 4% BSA. (**H**) Gene expression of PGC-1α in C2C12 myotubes exposed to IS (0 or 10 mg/dL, for 24 h) with media containing 4% BSA. Data are expressed as means ± SE. **P*<0.05 vs. 0 mg/dL of IS. PGC-1α, peroxisome proliferator-activated receptor gamma coactivator 1α.

Table 1. Animal characteristics

	Sham (n=12)	Sham +AST-120 (n=12)	CKD (n=12)	CKD +AST-120 (n=12)
Body and organ weights				
Body weight, g	29.6 ± 0.9	28.6 ± 0.6	29.8 ± 0.4	29.4 ± 0.5
Heart weight, mg	125 ± 7	120 ± 4	125 ± 4	123 ± 4
Quadriceps weight, mg	217 ± 10	212 ± 6	210 ± 8	218 ± 5
Gastrocnemius weight, mg	193 ± 7	191 ± 6	186 ± 2	187 ± 5
Soleus weight, mg	11.5 ± 0.4	10.9 ± 0.5	11.3 ± 0.5	11.2 ± 0.4
Hemodynamic measurements				
Systolic blood pressure, mmHg	121 ± 2	122 ± 3	119 ± 4	118 ± 3
Heart rate, bpm	548 ± 34	564 ± 19	559 ± 41	535 ± 37
Biochemical Measurements				
BUN, mg/dL	35 ± 2	34 ± 2	68 ± 4*	61 ± 2*
Total cholesterol, mg/dL	59 ± 3	54 ± 3	82 ± 2*	75 ± 2*
NEFA, mEq/L	0.7 ± 0.1	0.6 ± 0.1	0.6 ± 0.1	0.6 ± 0.1
Triglyceride, mg/dL	38 ± 4	37 ± 3	45 ± 6	46 ± 6
Fasting glucose, mg/mL	95 ± 6	96 ± 4	102 ± 7	91 ± 4
Hemoglobin, g/dL (n=8)	14.6 ± 0.4	14.2 ± 0.4	14.4 ± 0.6	14.2 ± 0.5

Values are means ± SE; CKD, chronic kidney disease; n, number of mice; bpm, beats per minute; BUN, blood urea nitrogen; NEFA, non-esterified fatty acid; *P<0.05 vs. Sham.

SUPPLEMENTAL FIGURE 1: (**A**) Blood glucose levels during intraperitoneal glucose tolerance test and area under the curve (AUC) of blood glucose levels during intraperitoneal glucose tolerance test in 4 groups of Sham, Sham+AST-120, CKD, and CKD+AST-120 mice (n=7-8 for each group). (**B**) Blood glucose levels during intraperitoneal insulin tolerance test and AUC of blood glucose levels during intraperitoneal insulin tolerance test in 4 groups of mice (n=7-8 for each group). Data are expressed as means ± SE.

SUPPLEMENTAL FIGURE 2: Renin-angiotensin system in 4 groups of Sham, Sham+AST-120, CKD, and CKD+AST-120 mice. (**A**) Plasma levels of angiotensin II in 4 groups of mice (n=10-12 for each group), (**B** and **C**) Representative western blot analysis (upper panel) and the summary data (lower panel) for AT1R and Gαq protein in the skeletal muscle from 4 groups of mice (n=9 for each group). Protein expression was normalized to GAPDH. Data are expressed as means ± SE. **P*<0.05 vs. Sham. AT1R, angiotensin II type 1 receptor.

SUPPLEMENTAL FIGURE 3: (**A**) Representative high-power photomicrographs of skeletal muscle tissue sections stained with CD31 and (**B**) The summarized data of $CD31^+$ capillary density from 4 groups of Sham, Sham+AST-120, CKD, and CKD+AST-120 mice (n=6 for each group). Scale bar=100 μm. Data are expressed as means ± SE.

Supplemental Table 1: Summary of echocardiographic analysis from 4 groups of Sham, Sham+AST-120, CKD, and CKD+AST-120 mice (n=4-5 for each group).

	Sham	Sham +AST-120	CKD	CKD +AST-120
LV EDD, mm	3.5 ± 0.1	3.4 ± 0.1	3.5 ± 0.1	3.5 ± 0.1
LV ESD, mm	2.3 ± 0.1	2.3 ± 0.1	2.4 ± 0.1	2.3 ± 0.1
Fractional shortening, %	33.4 ± 2.0	32.9 ± 0.8	32.7 ± 0.5	34.3 ± 1.2
AWT, mm	0.84 ± 0.01	0.81 ± 0.03	0.82 ± 0.02	0.80 ± 0.03
PWT, mm	0.82 ± 0.02	0.79 ± 0.02	0.79 ± 0.05	0.80 ± 0.02

Data are expressed as means ± SE; LV, left ventricular; EDD, end-diastolic diameter; ESD, end-systolic diameter; AWT, anterior wall thickness; PWT, posterior wall thickness.

Fig. 1

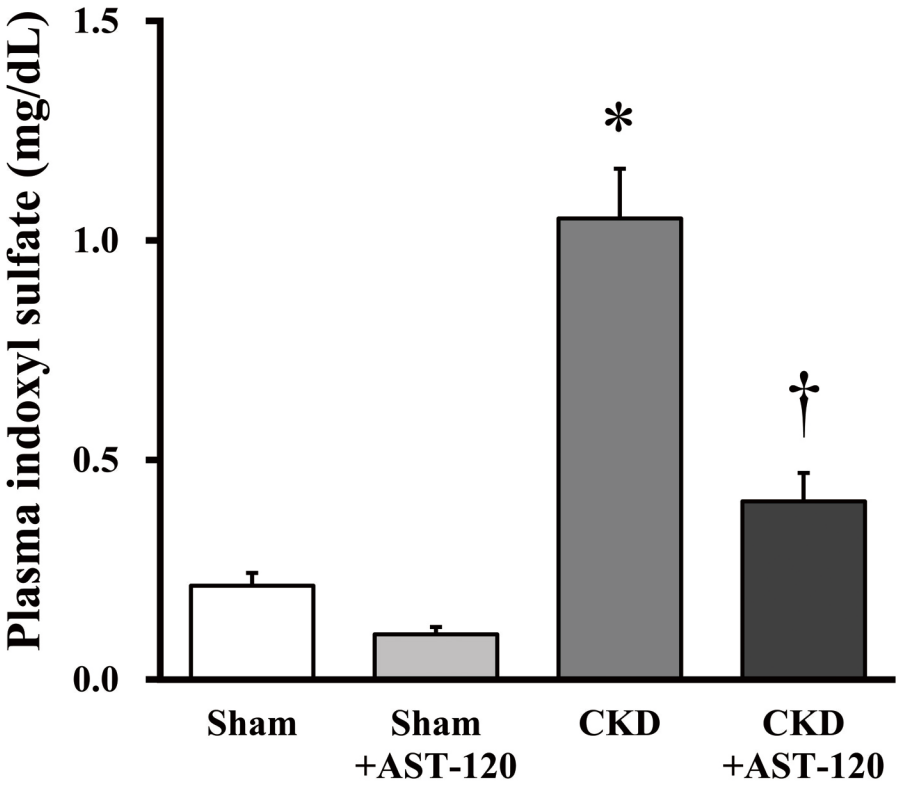
Plasma indoxyl sulfate (mg/dL)
1.5
1.0
0.5
0.0
*
†
Sham
Sham +AST-120
CKD
CKD +AST-120

Fig. 2

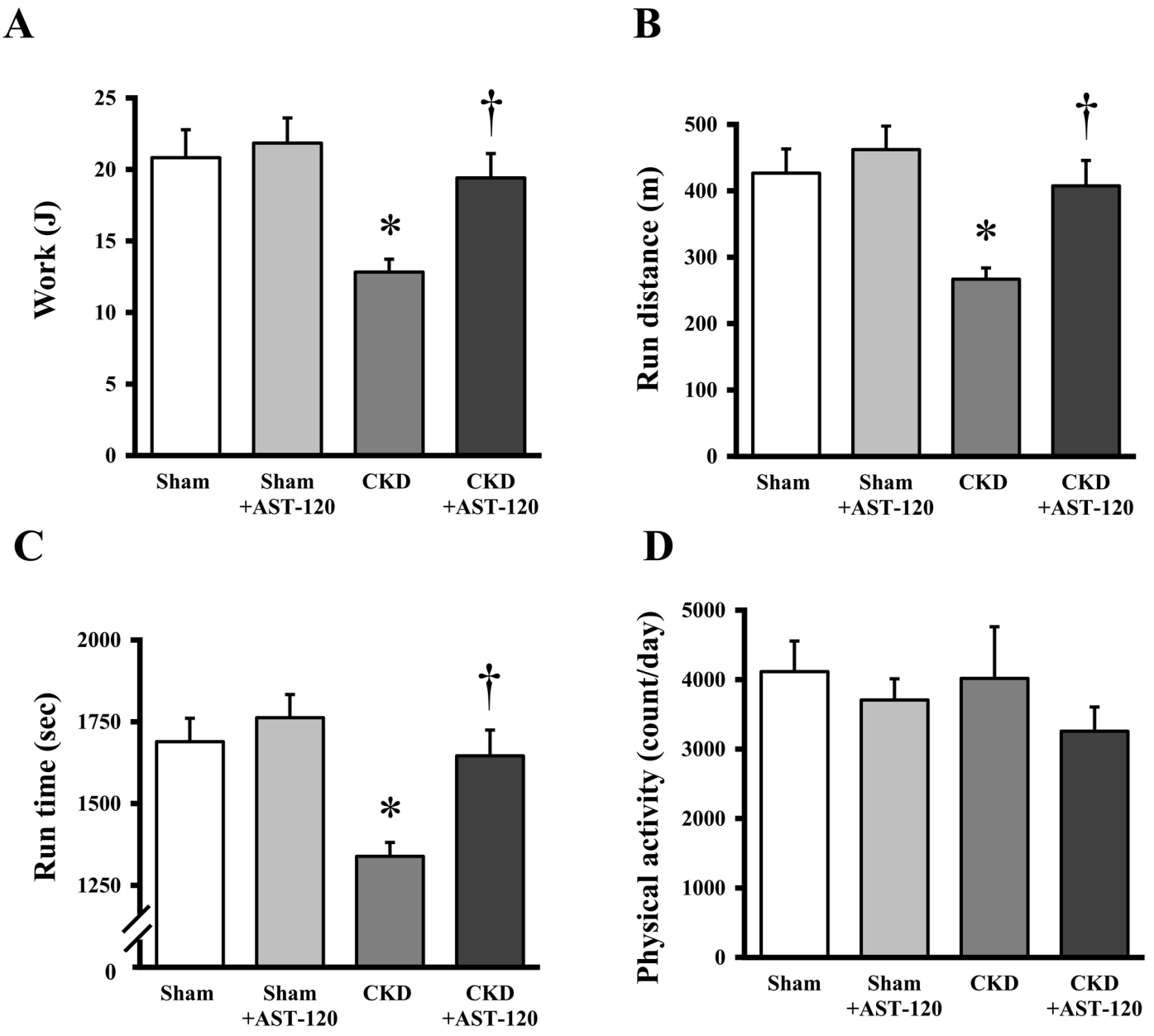
A
Work (J)
25
20
15
10
5
0
*
†
Sham
Sham +AST-120
CKD
CKD +AST-120
B
Run distance (m)
500
400
300
200
100
0
*
†
Sham
Sham +AST-120
CKD
CKD +AST-120
C
Run time (sec)
2000
1750
1500
1250
0
*
†
Sham
Sham +AST-120
CKD
CKD +AST-120
D
Physical activity (count/day)
5000
4000
3000
2000
1000
0
Sham
Sham +AST-120
CKD
CKD +AST-120

Fig. 3

A

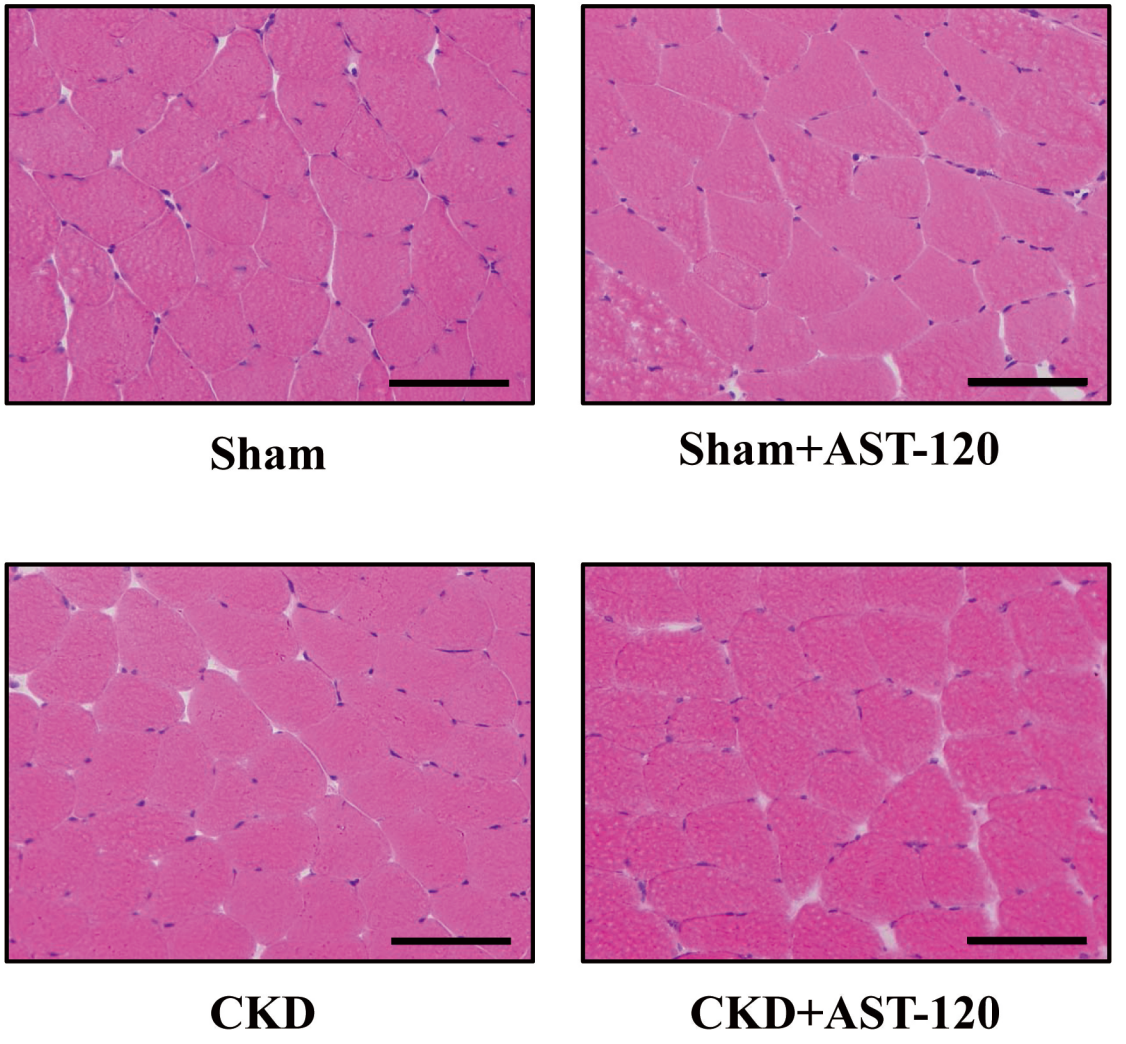
Sham
Sham+AST-120
CKD
CKD+AST-120

B

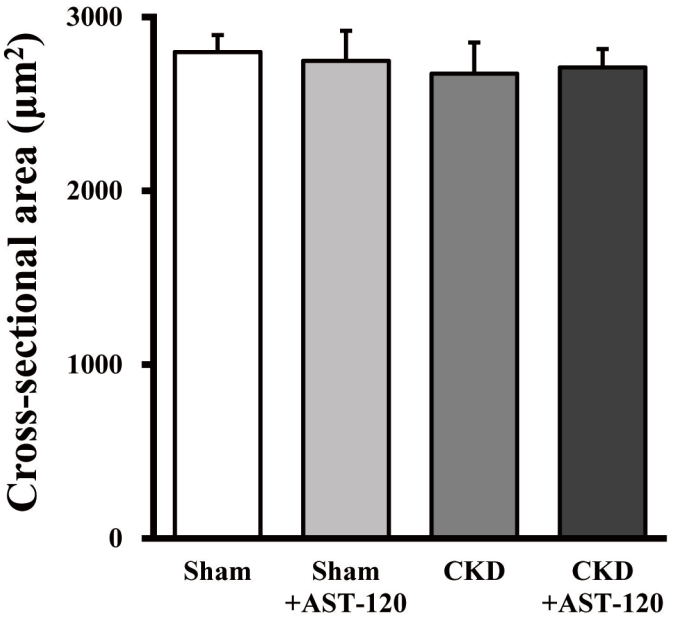
Cross-sectional area (μm²)
3000
2000
1000
0
Sham
Sham +AST-120
CKD
CKD +AST-120

Fig. 4

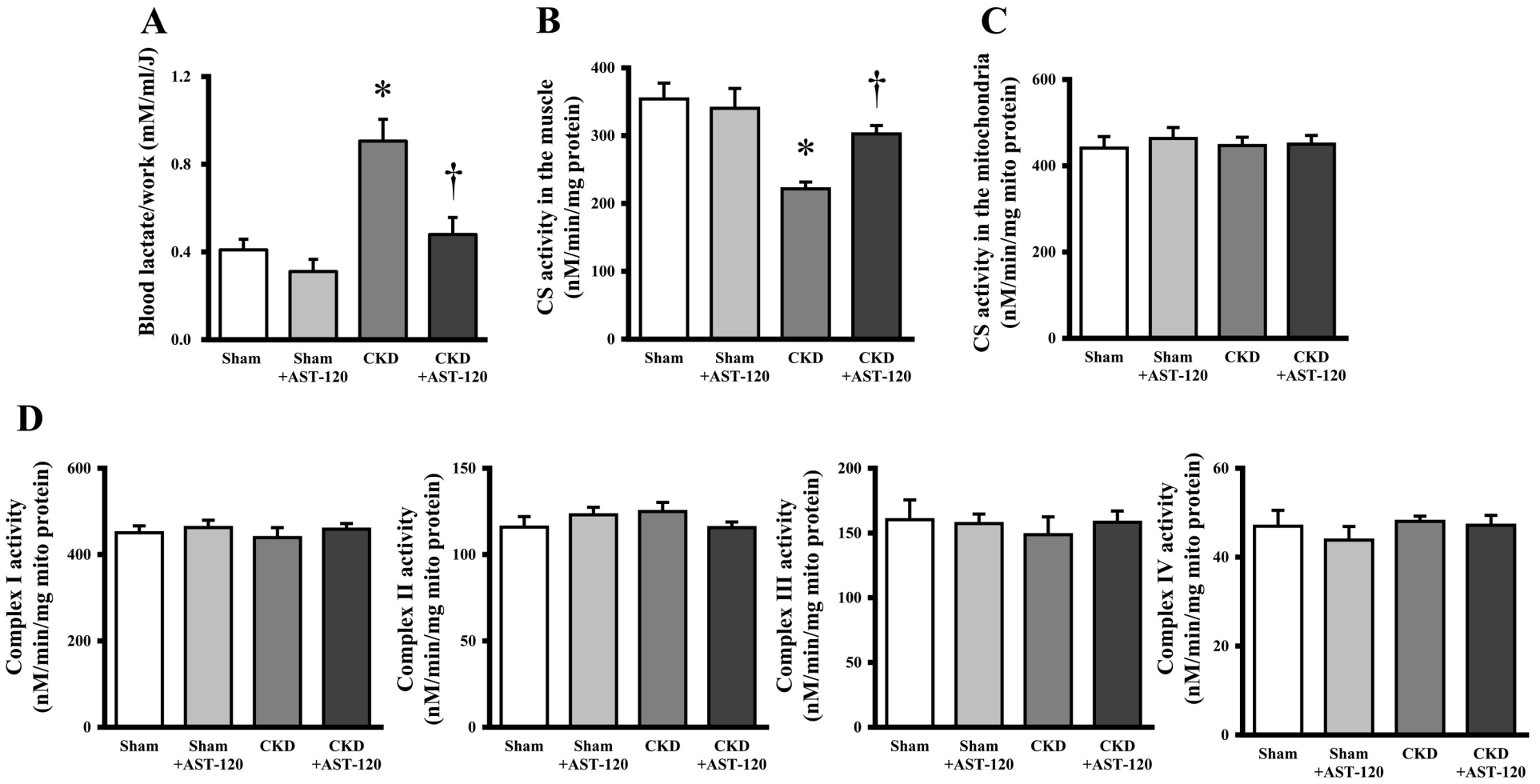
A
Blood lactate/work (mM/ml/J)
1.2
0.8
0.4
0.0
*
†
Sham
Sham +AST-120
CKD
CKD +AST-120
B
CS activity in the muscle (nM/min/mg protein)
400
300
200
100
0
*
†
Sham
Sham +AST-120
CKD
CKD +AST-120
C
CS activity in the mitochondria (nM/min/mg mito protein)
600
400
200
0
Sham
Sham +AST-120
CKD
CKD +AST-120
D
Complex I activity (nM/min/mg mito protein)
600
400
200
0
Sham
Sham +AST-120
CKD
CKD +AST-120
Complex II activity (nM/min/mg mito protein)
150
100
50
0
Sham
Sham +AST-120
CKD
CKD +AST-120
Complex III activity (nM/min/mg mito protein)
200
150
100
50
0
Sham
Sham +AST-120
CKD
CKD +AST-120
Complex IV activity (nM/min/mg mito protein)
60
40
20
0
Sham
Sham +AST-120
CKD
CKD +AST-120

Fig. 5

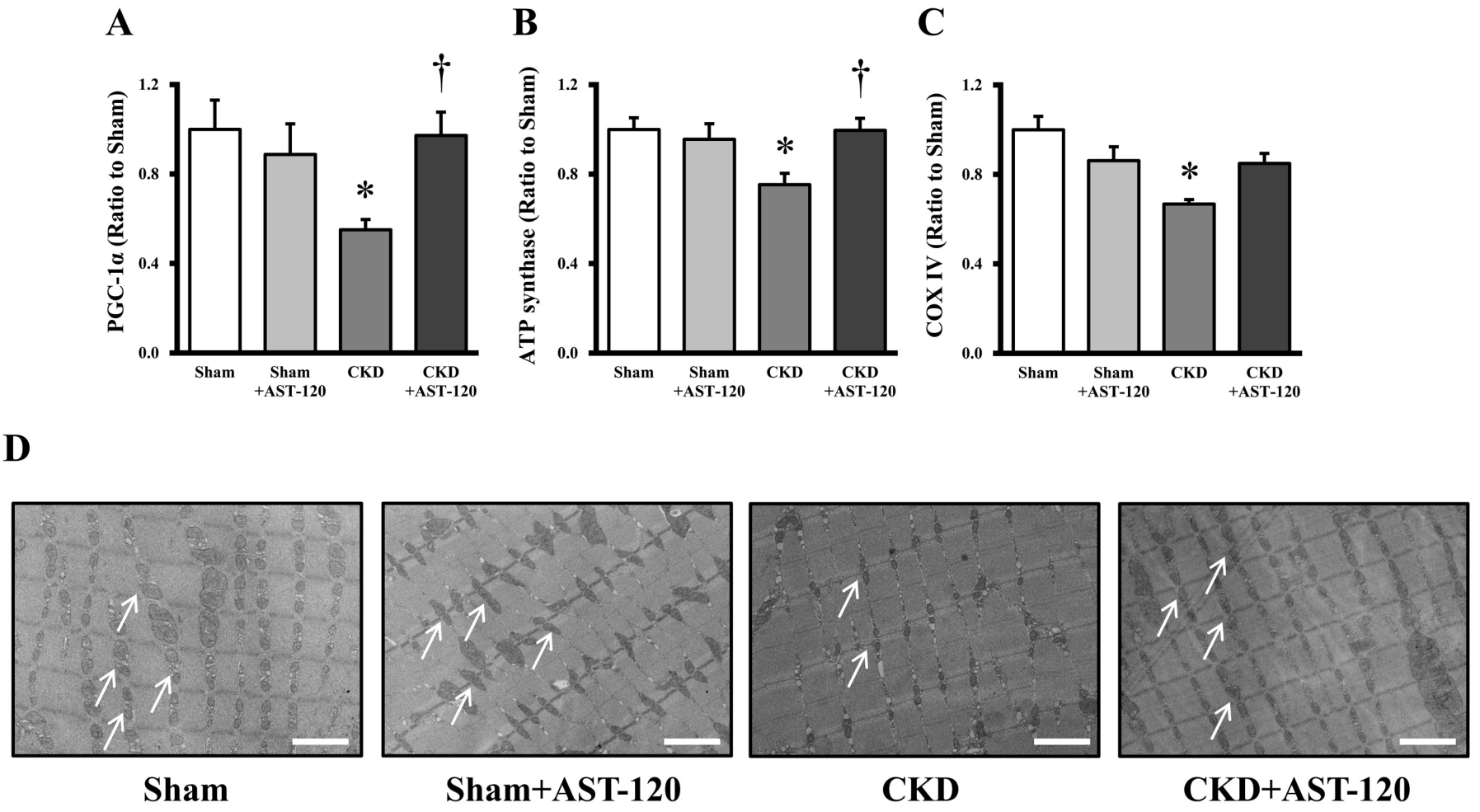
A
PGC-1α (Ratio to Sham)
1.2
0.8
0.4
0.0
*
†
Sham
Sham +AST-120
CKD
CKD +AST-120
B
ATP synthase (Ratio to Sham)
1.2
0.8
0.4
0.0
*
†
Sham
Sham +AST-120
CKD
CKD +AST-120
C
COX IV (Ratio to Sham)
1.2
0.8
0.4
0.0
*
Sham
Sham +AST-120
CKD
CKD +AST-120
D
Sham
Sham+AST-120
CKD
CKD+AST-120

Fig. 6

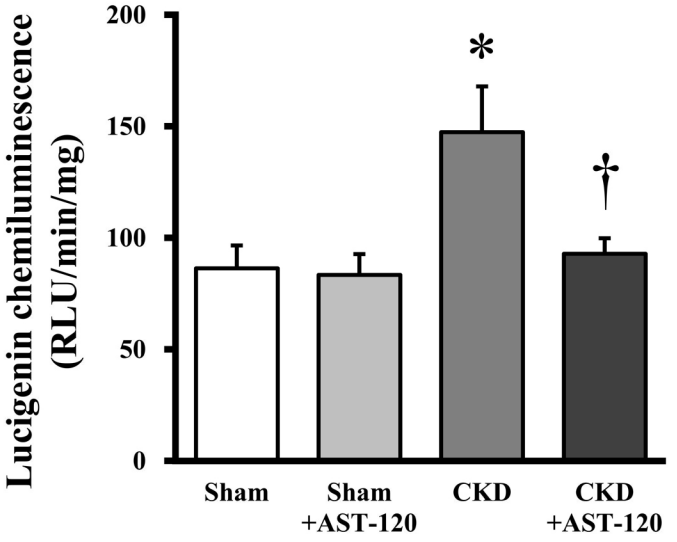
Lucigenin chemiluminescence
(RLU/min/mg)
200
150
100
50
0
*
†
Sham
Sham
+AST-120
CKD
CKD
+AST-120

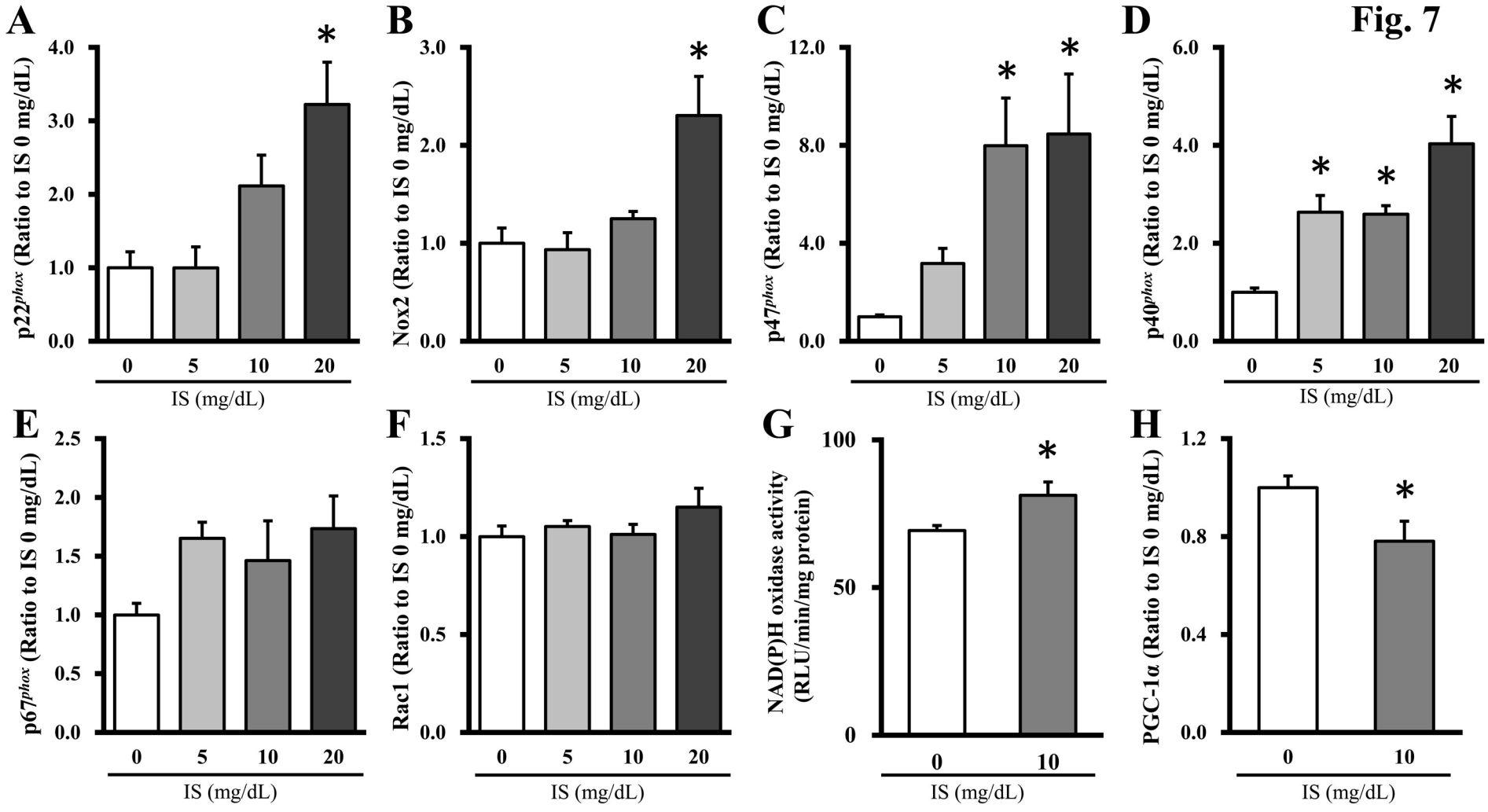
Fig. 7
A
p22phox (Ratio to IS 0 mg/dL)
4.0
3.0
2.0
1.0
0.0
*
0
5
10
20
IS (mg/dL)
B
Nox2 (Ratio to IS 0 mg/dL)
3.0
2.0
1.0
0.0
*
0
5
10
20
IS (mg/dL)
C
p47phox (Ratio to IS 0 mg/dL)
12.0
8.0
4.0
0.0
*
*
0
5
10
20
IS (mg/dL)
D
p40phox (Ratio to IS 0 mg/dL)
6.0
4.0
2.0
0.0
*
*
*
0
5
10
20
IS (mg/dL)
E
p67phox (Ratio to IS 0 mg/dL)
2.5
2.0
1.5
1.0
0.5
0.0
0
5
10
20
IS (mg/dL)
F
Rac1 (Ratio to IS 0 mg/dL)
1.5
1.0
0.5
0.0
0
5
10
20
IS (mg/dL)
G
NAD(P)H oxidase activity (RLU/min/mg protein)
100
50
0
*
0
10
IS (mg/dL)
H
PGC-1α (Ratio to IS 0 mg/dL)
1.2
0.8
0.4
0.0
*
0
10
IS (mg/dL)

Suppl Fig. 1

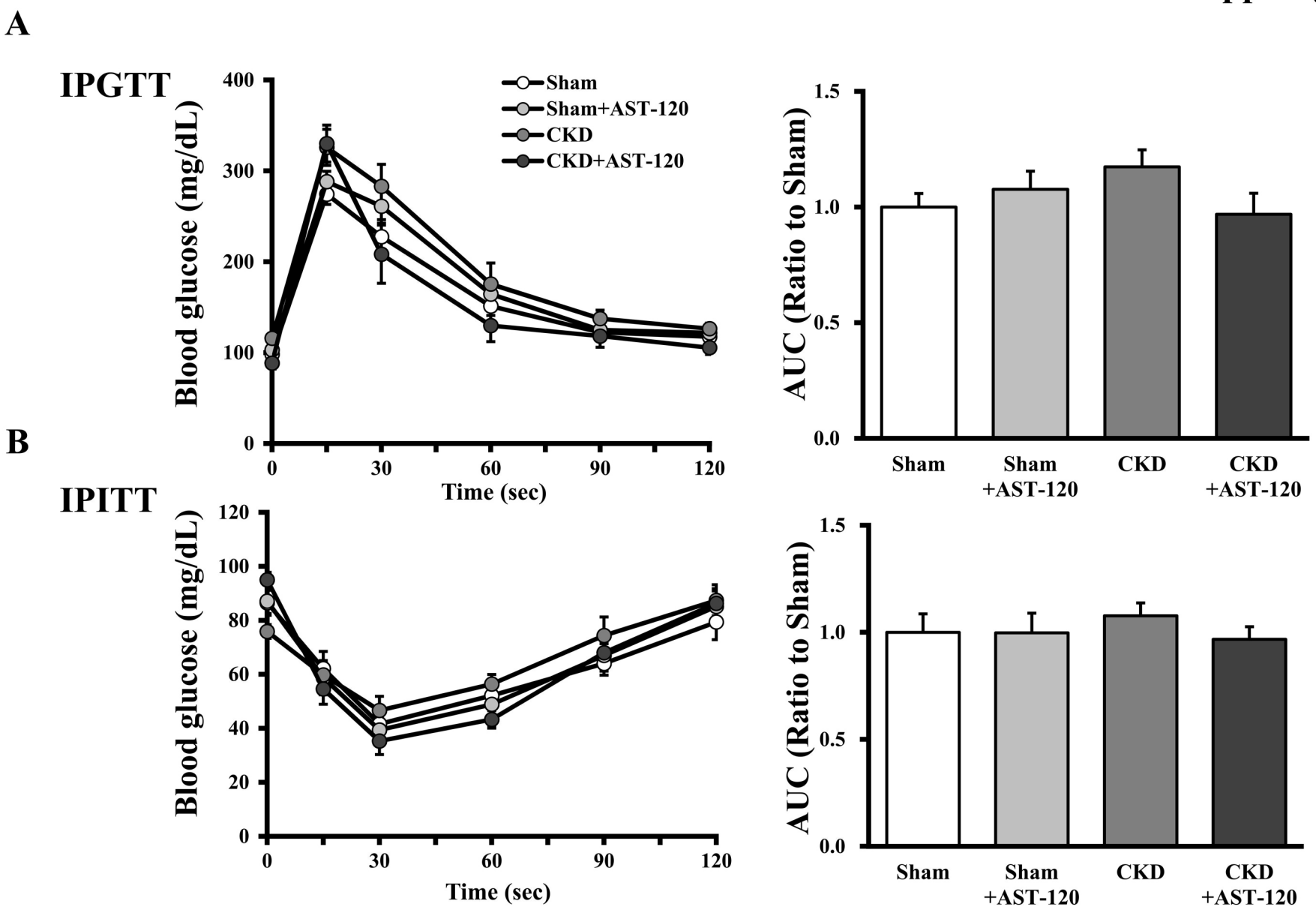
A
IPGTT
Blood glucose (mg/dL)
400
300
200
100
0
0
30
60
90
120
Time (sec)
Sham
Sham+AST-120
CKD
CKD+AST-120
AUC (Ratio to Sham)
1.5
1.0
0.5
0.0
Sham
Sham +AST-120
CKD
CKD +AST-120
B
IPITT
Blood glucose (mg/dL)
120
100
80
60
40
20
0
0
30
60
90
120
Time (sec)
AUC (Ratio to Sham)
1.5
1.0
0.5
0.0
Sham
Sham +AST-120
CKD
CKD +AST-120

Suppl Fig. 2

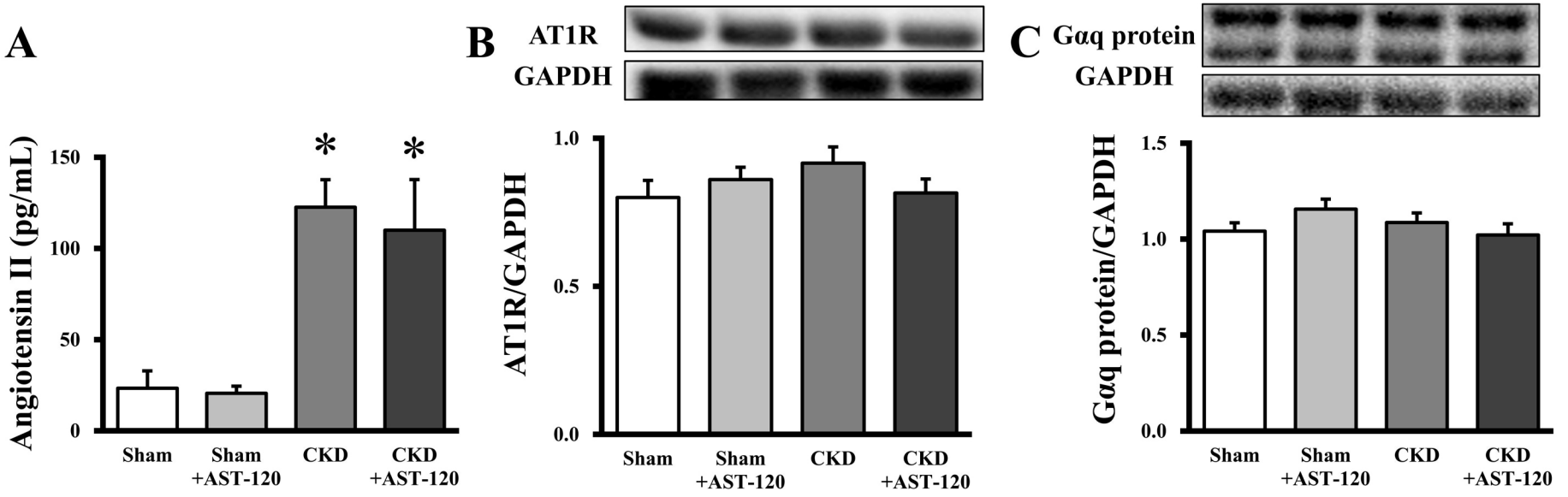
A
Angiotensin II (pg/mL)
150
100
50
0
*
*
Sham
Sham +AST-120
CKD
CKD +AST-120
B
AT1R
GAPDH
AT1R/GAPDH
1.0
0.5
0.0
Sham
Sham +AST-120
CKD
CKD +AST-120
C
Gαq protein
GAPDH
Gαq protein/GAPDH
1.5
1.0
0.5
0.0
Sham
Sham +AST-120
CKD
CKD +AST-120

A

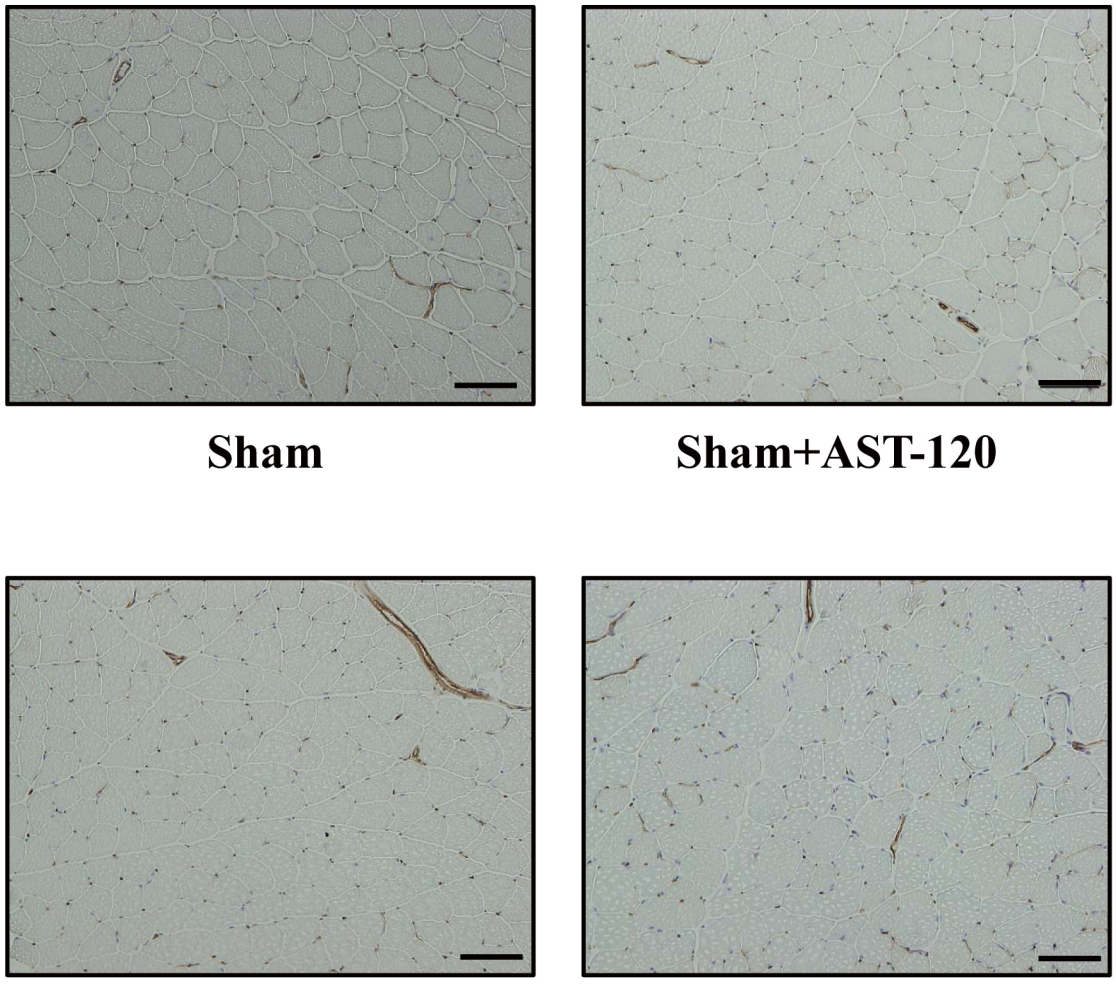
Sham
Sham+AST-120
CKD
CKD+AST-120

B

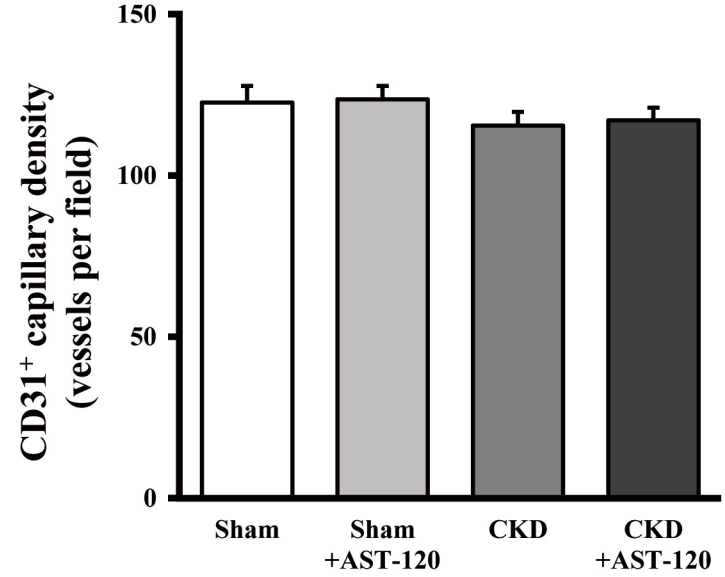
CD31+ capillary density
(vessels per field)
150
100
50
0
Sham
Sham
+AST-120
CKD
CKD
+AST-120